Original Research Paper

Anti-EpCAM functionalized graphene oxide vector for tumor targeted siRNA delivery and cancer therapy

Check for updates

Si Chen [a,b,c], Shuang Zhang [a,b,c], Yifan Wang [a,b,c], Xin Yang [a,b,c], Hong Yang [d,*], Chunying Cui [a,b,c,*]

[a] School of Pharmaceutical Sciences, Capital Medical University, Beijing 100069, China
[b] Engineering Research Center of Endogenous Prophylactic of Ministry of Education of China, Beijing 10069, China
[c] Beijing Area Major Laboratory of Peptide and Small Molecular Drugs, Beijing 10069, China
[d] Yanjing Medical College, Capital Medical University, Beijing 101300, China

ARTICLE INFO

ABSTRACT

Graphene oxide (GO) has emerged as a potential drug delivery vector. For siRNA delivery, GO should be modified to endow it with gene delivery ability and targeting effect. However, the cationic materials used previously usually had greater toxicity. In this study, GO was modified with a non-toxicity cationic material (chitosan) and a tumor specific monoclonal antibody (anti-EpCAM) for the delivery of survivin-siRNA (GCE/siRNA). And the vector (GCE) prepared was proved with excellent biosafety and tumor targeting effect. The GCE exhibited superior performance in loading siRNA, maintained stability in different solutions and showed excellent protection effect for survivin-siRNA *in vitro*. The gene silencing results *in vitro* showed that the mRNA level and protein level were down-regulated by 48.24% ± 2.50% and 44.12% ± 3.03%, respectively, which was equal with positive control ($P > 0.05$). It was also demonstrated that GCE/siRNA had a strong antitumor effect *in vitro*, which was attributed to the efficient antiproliferation, and migration and invasion inhibition effect of GCE/siRNA. The results *in vivo* indicated that GCE could accumulate siRNA in tumor tissues. The tumor inhibition rate of GCE/siRNA 54.74% ± 5.51% was significantly higher than control 4.87% ± 8.49%. Moreover, GCE/siRNA showed no toxicity for blood and main organs, suggesting that it is a biosafety carrier for gene delivery. Taken together, this study provides a novel design strategy for gene delivery system and siRNA formulation.

* Corresponding authors.
 E-mail addresses: yanghong@ccmu.edu.cn (H. Yang), ccy@ccmu.edu.cn (C. Cui).
 Peer review under responsibility of Shenyang Pharmaceutical University.

1. Introduction

RNAi has been a unique treatment of genetic diseases, such as malignant tumors [1], cardiovascular diseases [2], hypertension [3], diabetesm [4]. *In vivo*, double-stranded RNA (dsRNA) is firstly degraded to small interfering RNA (siRNA) by the specific enzymes. And then, siRNA associates mRNA according to the principle of base complementation, so as to induce the process of downregulating its expression [5,6]. However, it is difficult to introduce exogenous siRNA into the body and produce specific therapeutic effects in treatment position [7]. There are many limitations for the successful application of siRNA *in vivo*, such as half-life, high molecular weight, negative charge, hydrophilicity, instability, degradation and filtration by glomerul, etc. [8,9]. It is urgent to develop an effective delivery carrier for introducing exogenous siRNA into the body and producing specific therapeutic effects at the therapeutic site.

For efficient gene delivery, it is essential to load gene drugs into a delivery vector, which is divided into viral vector and non-viral vector. The further clinical application of viral vectors is limited due to the biological safety problems such as cytotoxicity, high immunogenicity and potential carcinogenicity [10,11]. At present, non-viral gene delivery vectors such as cationic polymers [12], cationic polysaccharides [13], protamine [14], cationic lipids [15] and cationic surfactants [16] have become the focus of gene therapy research due to low toxicity, low immunogenicity, *etc*. Unfortunately, the transfection efficiency of non-viral vectors is not ideal *in vivo*. Therefore, it has become the most urgent and challenging topic in gene therapy to search a new non-viral vector with high efficiency and low toxicity.

Graphene oxide (GO) is a derivative of graphene, which is a carbon material with two-dimensional (2D) honeycomb structure formed by accumulation of single-layer sp^2 hybridized carbon atoms [17–19]. There are a lot of oxygen functional groups (carboxyl, hydroxyl, epoxy) on the surface and edges of GO, and large conjugated structure is convenient to covalent and non-covalent functionalization [20–22]. In recent years, GO has attracted more and more attention in the area of biomedical research and application due to its high water dispersibility, colloidal stability, large specific surface area and surface modification. Many studies have proved that GO can be widely used in the application of drug and gene carriers [23,24], cell imaging [25], biosensor [26] and antibacterial materials [27] for the treatment and diagnosis of diseases. It is necessary to modify GO properly to ensure the gene loading ability and targeting effect of GO.

As a natural alkaline polysaccharide with positive charge [28], chitosan (CS) has many advantages, such as non-toxicity, good biocompatibility and biodegradability, making it an excellent material for gene delivery. Therefore, CS was selected for the modification of GO in this research. As an inorganic-organic hybrid nanoparticle, the CS modified GO is supposed to be a versatile platform for gene delivery, which has the advantages of both inorganic and organic materials [29–32]. Epithelial cell adhesion molecule (EpCAM) is a type I transmembrane glycoprotein which is normally expressed only on the basement membrane of epithelial tissue except squamous epithelium [33]. EpCAM is only localized in the basement membrane of epithelial tissue in normal tissues. In pathological cases, EpCAM is usually expressed in inflammatory area and epithelial cells with rapid proliferation. EpCAM is highly expressed in adenocarcinoma, including lung cancer, pancreatic cancer, breast cancer, ovarian cancer *etc.* [34–36]. As reported previously [37], EpCAM was abundantly expressed in breast cancer cells, which was 100–1000 times higher than that in normal tissue cells. EpCAM monoclonal antibody (anti-EpCAM) is a specific antibody for highly expressed EpCAM molecule on the surface of cancer cells.

In this study, CS was conjugated onto the GO surface through amide bonds (GO–CS), and then anti-EpCAM was connected with GO–CS by π-π interaction. A novel carrier GO–CS/anti-EpCAM (GCE) for siRNA delivery was successfully prepared. Survivin-siRNA was applied to explore the siRNA delivery by GCE. Silencing of survivin inhibits the development and metastasis of tumors by promoting apoptosis, and arrests the tumor cells at G0/G1 phase. The results showed that GCE could effectively encapsulate survivin-siRNA and inhibit the proliferation of MCF-7 breast cancer cells, producing significant anti-tumor effects *in vitro* and *in vivo* (Scheme 1). It is believed that the antibody functionalized graphene oxide material can serve as a promising gene delivery vector, and has a broad clinical application prospect in the future.

2. Materials and methods

2.1. *Materials*

Graphene oxide, chitosan (Mw = 50 kDa), chloroacetic acid, 2-(N-morpholino) ethanesulfonic acid (MES, 99%), N-(3-dimethylaminopropyl)-N′-ethylcarbodiimide hydrochloride (EDC•HCl, 99%) and N-hydroxysuccinimide (NHS, 98%) were purchased from Sigma-Aldrich (St Louis, USA). Anti-EpCAM antibodies (anti-EpCAM) produced in mouse was obtained from Abcam (Cambridge, UK). MCF-7 cell line was obtained from the Cell Bank of Chinese Academy of Sciences. Homo-survivin-siRNA, FAM-survivin-siRNA, Cy5-survivin-siRNA, and the negative control siRNA (NC) were purchased from GenePharma Co., Ltd. (Shanghai, China). Lipo^{TM}2000 (Lipo), Hoechst 33,342, TRIzol and Alexa Fluor® 488 annexin V/Dead Cell Apoptosis Kit was purchased from Invitrogen (Carlsbad, USA). RPMI-1640 medium and trypsin were purchased from Hyclone Laboratories Inc. (Logan, USA). Fetal bovine serum (FBS) was purchased from GIBCO (Grand Island, USA). High Capacity RNA-to-cDNA Kit, High Capacity cDNA Reverse Transcription Kit, TaqMan Gene Expression Master Mix TaqMan Gene Expression Assays (survivin assay, GAPDH assay), and human survivin ELISA kit were bought from Thermo Fisher Scientific (Waltham, USA). DAPI and doxorubicin hydrochloride (DOX•HCl) was purchase from Sigma-Aldrich (St Louis, USA). Matrigel was purchased from BD Biosciences (New Jersey, USA).

MCF-7 human breast tumor cells were cultured in RPMI-1640 medium containing 10 FBS, 1% penicillin and streptomycin, and kept at 37 °C with 5% CO_2. The cells
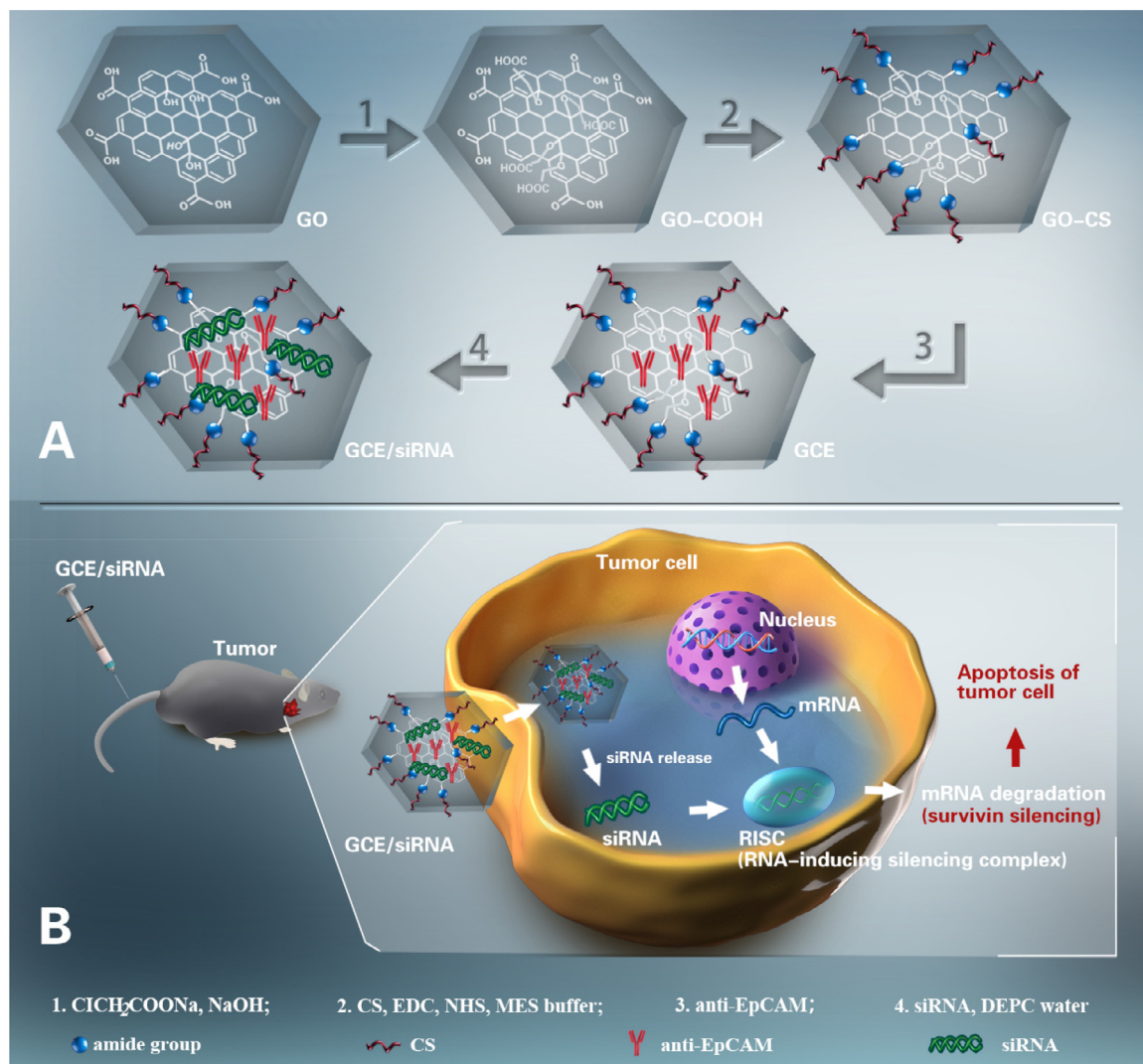
Scheme 1 – Schematic illustration of mechanisms and preparation of GCE/siRNA. (A) GCE/siRNA were prepared by GO-COOH, functionalization with chitosan (GO-CS), immobilization with anti-EpCAM (GCE) and then mixing with survivin-siRNA (GCE/siRNA) in aqueous solution. (B) After targeted into tumor tissues, GCE could deliver survivin-siRNA into cells successfully, and survivin-siRNA could release from GCE/siRNA to perform the antitumor effect.

were subcultured 2,3 times a week till they reached 80% confluence.

Specific pathogen free (SPF) female BALB/c nude mice (4–6 weeks, 15–17 g) were purchased from Animal Department of Capital Medical University (Beijing Laboratory Animal Center, Beijing, China). The guideline for all of the animal experiments was the Laboratory Animal-Guideline for Ethical Review of Animal Welfare issued by the National Standard GB/T 35,892–2018 of the People's Republic of China.

2.2. Synthesis of GO-CS

In order to attach CS with GO more effectively, the hydroxyl, epoxide, and the carbonyl groups of GO were converted to carboxyl group. As shown in Fig. 1, carboxylic acid-functionalized GO (GO-COOH) was synthesized by oxidation method [38,39]. Firstly, GO (50 mg) was added to 30 ml water

and sonicated for 2 h to disperse homogeneously. Then, NaOH (5 g) and $ClCH_2COONa$ (5 g) were added to the suspension. After ultrasonic reaction for 2 h, the reaction was stirred at room temperature for 3 h. Then, the supernatant was discarded after centrifugation (10 000 × g, 4 °C) for 10 min, and the precipitation was washed by water for 3 times. The product was freeze dried for 48 h to obtain GO-COOH. GO-CS was prepared by a typical method. GO-COOH (20 mg) and CS (140 mg) were dispersed in 10 ml of MES buffer (0.1 M, pH 5) and the suspension was sonicated for 1 h. EDC (300 mg) and NHS (300 mg) were slowly added into the mixture and sonicated for 6 h. Then the reaction was stirred at room temperature for 16 h, and the supernatant was discarded after centrifugation (10 000 × g, 4 °C) for 60 min. The sediment was washed by 1% acetic acid, and then washed with water for 3 times [40]. GO-CS was obtained after 48 h of freeze-drying.
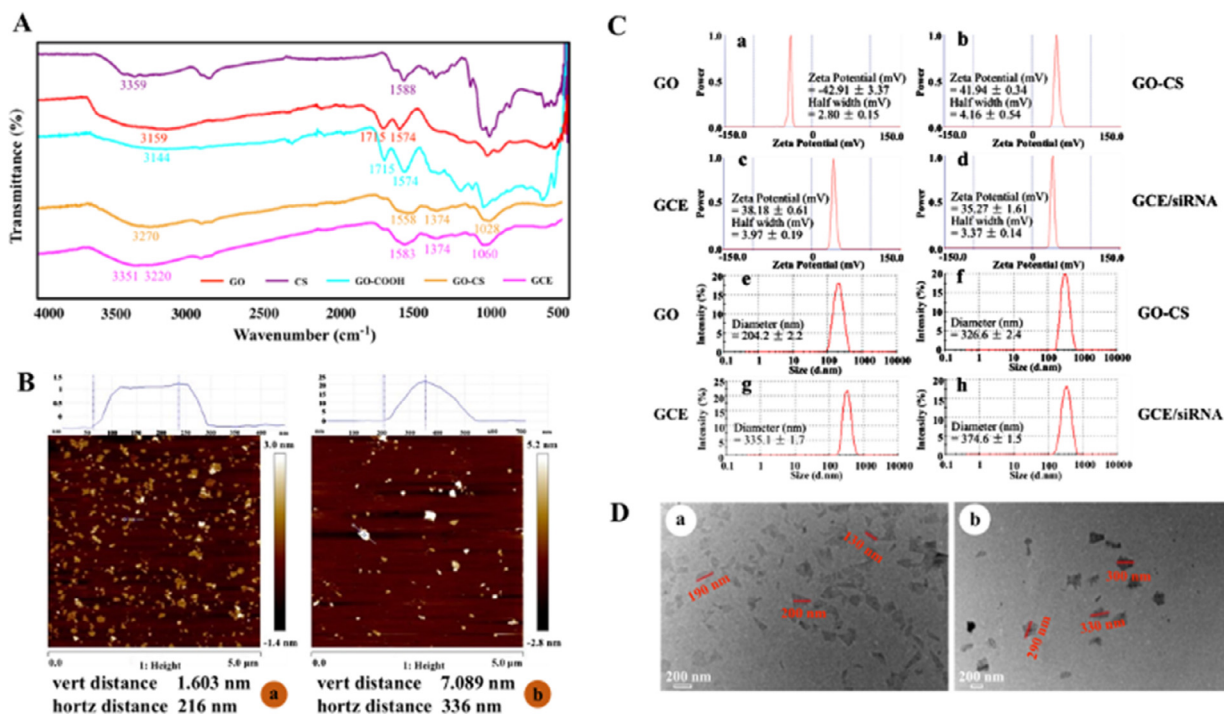
Fig. 1 – Characterization of GCE/siRNA. (A) The chemical structure of GO, CS, GO-COOH, GO-CS and GCE were determined by FTIR spectra. (B) AFM images of GO (a) and GCE (b). (C) The zeta potential value of GO (a), GO-CS (b), GCE (c) and GCE/siRNA (30:1, w/w) (d), the particle size of GO (e), GO-CS (f), GCE(g) and GCE/siRNA (30:1, w/w) (h). (D) TEM of GO (a) and GCE (b). The data were presented as the mean ± SD, $n = 3$ (For interpretation of the references to color in this figure, the reader is referred to the web version of this article.).

2.3. Immobilization of GCE

In order to increase the targeting effect of gene vectors, EpCAM monoclonal antibody (anti-EpCAM) was immobilized onto the surface of GO-CS. Briefly, GO-CS (3 mg) was evenly dispersed in 3 mL water. Anti-EpCAM (6 μg) was added and stirred overnight at room temperature. The supernatant was discarded after centrifugation (10 000 × g, 4 °C) for 1 h, and the sediment was washed with water for 3 times [41]. GCE was obtained after 48 h of freeze-drying.

2.4. Preparation of GCE/siRNA

GCE/siRNA complex was prepared as follows: 1 OD survivin-siRNA (33 μg) was dissolved in 250 μl of fresh diethylpyrocarbonate (DEPC) water to obtain 10 μmol/l survivin-siRNA solution. GCE solution (1 mg/ml) and survivin-siRNA solution were mixed at a series of mass ratios, and the transfection complex GCE/siRNA could be obtained after the reaction solutionsgently shaken and incubated at room temperature.

2.5. Characterization of GCE

The structure of the GO, GO-CS and GCE were determined by FTIR spectra (Nicolet iS5, USA) and UV absorption spectra (UV-2600, Kyoto, Japan). The morphology of GO and GCE were observed by transmission electron microscope (TEM, Tokyo, Japan). Atomic force microscopy (AFM) images were gotten by atomic force microscopy (Veeco Instruments Inc., USA). The hydrodynamic size of GCE/siRNA was obtained by Zetasizer Nano ZS (Malvern Instruments Ltd, UK) at room temperature. Zeta potentials were measured by a zeta potential machaine (ZetaPlus, Brookhaven, USA).

2.6. Agarose gel retardation assay

Agarose gel retardation assay was applied to the detection of loading capacity of GCE and ratio of GCE to survivin-siRNA. GCE/siRNA complex was prepared at a certain mass ratio (2–50, w/w). Each complex (10 μl) at different proportions was carefully added to the hole of the agarose gel (1% agarose gel with 10 mg/ml EtBr) in Tris/Borate/EDTA (TBE) buffer, respectively. After electrophoresed under 120 V for 30 min, the siRNA bands were imaged by a UV transilluminator (Geliance 600, PerkinElmer Inc., Waltham, USA).

2.7. Anti-RNase a degradation assay

Survivin-siRNA (1 μg) and GCE/siRNA loaded with survivin-siRNA (1 μg) (w/w = 30:1) were mixed with RNase A solution (0.1 mg/ml) separately at 37 °C for 0.5 h. EDTA (5 μl, 5 mM) was added at the determined time point. Then, 20 μl, 0.8 mg/ml of heparin sodium was added at 37 °C for 0.5 h to replace survivin-siRNA protected by GCE vector. The samples at

different time points were operated according to the agarose gel retardation assay mentioned above.

2.8. Cellular uptake

FAM-labeled survivin-siRNA were performed in the experiment. After seeded for 24 h, MCF-7 cells were treated with siRNA (100 nM), GCE/siRNA (contain 100 nM siRNA), and Lipo/siRNA (contain 100 nM siRNA), respectively. After incubation and transfection for 5 h, each medicinal medium was discarded and washed by PBS solution for 3 times. Hoechst 33,342 (1 ml, 1 µg/ml) was added into the well. After incubation for 15 min, the staining solution was discarded and the cells were washed 3 times by PBS. The cellular uptake results were observed by confocal microscopy (CLSM, TCSSP5, Leica, Wetzlar, Germany).

2.9. Cell toxicity assay

MTT assay was performed to evaluate the toxicity of GCE against MCF-7 cells. MCF-7 cells (5×10^3 cells/well) were seeded and incubated for 24 h. The cells were treated with GCE at various concentrations (10–150 µg/ml). After incubation for 2 d, 25 µl, 5 mg/ml of MTT was added and the cells were incubated at 37 °C with 5% CO_2 for 4 h. The absorbance of each well was tested by microplate reader (EnSpire, PerkinElmer Inc., USA), and the detection wavelength was 570 nm.

The antitumor activity of different complexes *in vitro* was also tested by MTT test. The cells were treated respectively with naked NC, naked siRNA, GCE/NC, GCE/siRNA, Lipo/NC, Lipo/siRNA (containing 20, 40, 80, 120 and 160 nM siRNA).

2.10. Real-time PCR

After MCF-7 cells were transfected for 2 d, TRIzol reagent (2 ml) was used to extract the RNA from each group, and then the RNA concentration was measured by Nanodrop 1000 spectrophotometer. 2 µg of total RNA of MCF-7 cells was reverse transcribed to cDNA, and then cDNA was transcribed to survivin-mRNA with housekeeping gene GAPDH as an internal control. The value relative quantity of survivin-mRNA expressions were calculated with average threshold cycle (Ct) by the delta-delta Ct ($2^{-\Delta\Delta Ct}$) test.

2.11. ELISA

MCF-7 cells were incubated and transfected for 2 d By the end of culture, the cells were collected and lysed with RIPA buffer. The protein concentration and survivin-protein were calculated by a BCA protein kit and a human survivin ELISA kit, respectively. Plates were read at 450 nm to measure the OD values.

2.12. Apoptotic cell morphology

3×10^5 cells of MCF-7 cells were seeded in a 20 mm dish and incubated for 1 d. The cells were treated with siRNA (100 nM survivin-siRNA), GCE/NC (contain 100 nM NC-siRNA), GCE/siRNA (contain 100 nM survivin-siRNA) for 2 d,

respectively. The cells were washed 3 times by PBS. 10% formalin stationary solution was added for 20 min. Then, the cells were stained with DAPI (1 ml, 1 µg/ml) at 37 °C, 5% CO_2 incubator for 8 min. After staining, the cells were washed by PBS solution, and the apoptotic morphology was observed and photographed by CLSM.

2.13. Analysis of cell cycle and apoptosis rate by FCM

After MCF-7 were incubated and treated with GCE/NC (contain 100 nM NC-siRNA) and GCE/siRNA (contain 100 nM survivin-siRNA) for 2 d, the cells were collected and washed by cold PBS solution, respectively. Then the cells were resuspended by adding binding buffer (250 µl, 1×) to a concentration of 1×10^6 cells/ml. According to instructions of Cell Apoptosis Kit, Alexa Fluor® 488 annexin V (5 µl) and PI (1 µl, 100 µg/ml) were added (100 µl), respectively. The cells were incubated for 15 min in darkness at room temperature, and then binding buffer (400 µl, 1×) was added. The apoptosis rate of MCF-7 cells in each group was calculated by a flow cytometry (BD LSRFortessa, Becton Dickinson, USA) immediately.

2.14. Wound healing assay

Wound healing assay is a commonly used method to evaluate the migration ability of cancer cells [42,43]. MCF-7 (4×10^5 cells/well) were seeded and incubated until the cell confluence reached 90%–100%. Then, in order to simulate the wound formation, the 10 µL micropipette tip was used to scratch vertically at each well of the 6-well plate to ensure that the four to five straight lines. MCF-7 cells were incubated and treated with GCE/NC (containing 100 nM NC-siRNA) and GCE/siRNA (containing 100 nM survivin-siRNA). The scratch widths of cells in each group were observed at determined time points (0, 24 and 48 h) by a fluorescence microscopy (Nikon Eclipse Ti, Tokyo, Japan).

2.15. Transwell assay

Migration assay of the MCF-7 cells was quantified by the cells that directionally migrated through 8 µm pore size polycarbonate filter of the transwell chamber (Corning Inc., NY, USA) [44]. The MCF-7 cells of each group were suspended with serum-free RPMI-1640 containing 0.1% BSA. The cells (100 µl, 2×10^5/ml) were seeded in the upper chamber, while RPMI-1640 medium containing 10% FBS (600 µl) was added into the lower chamber. After incubated for 24 h, the culture medium was discarded from the transwell chamber, then the non-migrating cells were carefully wiped from the upper chamber, and the upper chamber was washed twice with PBS. Then the cell was fixed, stained, and washed by PBS. After air-dried naturally, the transwell chamber was turned upside down and placed on the slide under a fluorescent microscopy (DM6000B, Leica, Wetzlar, Germany). Five visual fields were randomly selected for photography (× 200). The invasion test was carried out, except that the upper surface of the filters was covered with matrigel in serum-free RPMI-1640 medium at 4 °C.

2.16. Distribution of GCE/siRNA in vivo

In order to explore the targeting and organ distribution of GCE in nude mice, a model of human breast cancer xenograft in nude mice was established. MCF-7 cells (1×10^7 cells/mouse) were subcutaneously injected into mouse. After 20 d, the tumor volumes was approximately 100 mm^3. The mice were randomly divided into four groups, which were injected with normal saline (NS), naked Cy5-siRNA (0.3 mg/kg), GC/Cy5-siRNA (contain 0.3 mg/kg siRNA) and GCE/Cy5-siRNA (contain 0.3 mg/kg siRNA) into tail vein respectively. The nude mice were imaged after injection for 1, 2, 4 and 8 h. After observation, all of the mice were sacrificed and the main organs (hearts, livers, spleens, lungs and kidneys) were dissected. The fluorescence distribution in organs was photographed by an *in vivo* fluorescence system (IVIS Spectrum, USA).

2.17. Tumor inhibition assay and toxicity study in vivo

The nude mice with MCF-7 cell transplantation tumor model were divided into 4 groups ($n = 6$), and treated respectively with NS, naked siRNA (0.3 mg/kg), GCE/siRNA (containing 0.3 mg/kg siRNA), and DOX (1.2 mg/kg) every other day for 5 times. On the last injection, all mice were sacrificed and the tumors and the main organs of each group were collected to study tumor inhibition and organ toxicity *in vivo*. The histomorphological structure changes of organs and tumor tissues were observed by H&E staining.

2.18. Hemocompatibility test

The fresh rat blood (5 ml) was centrifuged (2 000 × g, 10 min), and washed by PBS for 3 times to obtain the red-blood-cell (RBC). Then, 2% (v/v) RBC suspension was prepared with PBS solution. Naked siRNA, GCE, GCE/siRNA and Lipo/siRNA (100 µl) with a series of concentrations were mixed with 2% RBC suspension (900 µl). After incubation for 1 h at 37 °C, the samples were centrifuged (3 000 × g, 10 min). The absorbance was measured at 540 nm.

2.19. Blood biochemistry test

Hematological examination was performed to explore the potential toxicity of drugs *in vivo*. BALB/c nude mice were divided into four groups ($n = 5$), and injected by NS, naked siRNA (0.3 mg/kg), GCE/siRNA (containing 0.3 mg/kg siRNA), and DOX (1.2 mg/kg) every other day for 5 times. After the drug administration, blood samples were collected from all nude mice, and blood routine test was performed by an automatic hematology analyzer (MEK6400, Nihon Kohden, Japan).

The whole blood was taken from the blood collection vessel without anticoagulant for blood biochemical examination. The whole blood was kept at room temperature for 2 h, and centrifuged (3 000 × g, 4 °C) for 10 min to obtain the upper serum. The important blood biochemical indicators of liver function (ALT: alanine aminotransferase, AST: aspartate aminotransferase, ALP: alkaline phosphatase, TB: total protein, and ALB: albumin) and renal function (CREA: creatinine, UA: uric acid, and UREA) of nude mice were detected by an automatic biochemical analyzer (BS-350E, Mindray, China).

2.20. Statistics

Data were represented as the Mean ± SD. The results were treated statistically by paired two-sample Student's *t*-test. A value of $P < 0.05$ was considered statistically significant, and a value of $P < 0.01$ was considered very significant.

3. Results and discussion

3.1. Synthesis and characterization of GCE

The novel siRNA vector GCE was prepared as described in Scheme 1A. The chemical structure of GCE nanoparticles was confirmed by FTIR (Fig. 1A) and UV spectroscopy (Fig. S1). Compared with the FTIR spectrum of GO-COOH (blue), there was a characteristic peak of C-N group at 1374 cm^{-1} in that of GO-CS (yellow), and the $C=O$ stretching vibration peak shifted from 1574 cm^{-1} to 1558 cm^{-1}. These results indicated that CS was successfully grafted onto GO-COOH surface. When compared the spectra of GO-CS and GCE (pink), the $C=O$ stretching vibration peak shifted from 1558 cm^{-1} to 1583 cm^{-1}, and the absorption peak became stronger in the spectrum of GCE, which indicated that anti-EpCAM was successfully modified on GO-CS and GCE composite. The thermal stability of GO was also different when compared with GO-CS, GCE and siRNA loaded GCE, which further confirmed the successful preparation of GCE/siRNA (Figs. S2 and S3).

The structures of GO and GCE were observed by AFM (Fig. 1B) and TEM (Fig. 1D). The diameter of unmodified GO was in the range of 70–280 nm, while the diameter of GCE increased to 80–350 nm. The thickness was also increased after modification. These results indicated that CS and anti-EpCAM had been successfully modified on the surface of GO. Meanwhile, the edges of GO particles are sharper but thinner than that of GCE particles, mainly due to the packaging and folding of polymer CS. The average hydrodynamic radius and zeta potential of GO, GO-CS, GCE and GCE/siRNA nanoparticles were determined by DLS (Fig. 1C). In our previous research, GO was decorated with cationic materials such as octaarginine (R8) and poly-L-lysine (PLL) for siRNA delivery [45–47]. The zeta potential of CS functionalized GO was (41.94 ± 0.34) mV (Fig. 1C), which is even more positive than R8 or PLL functionalized GO. This character makes GO-CS a promising vector for siRNA.

3.2. Drug loading and stability analysis

GCE/siRNA nanoparticles at the different weight ratios (2:1, 5:1, 10:1, 20:1, 30:1, 40:1, and 50:1) were prepared. In the group of GO/siRNA, the bright siRNA bands were observed at all ratios. While in GCE/siRNA group, the bands of GCE/siRNA disappeared completely when the ratio reached 30:1 (Fig. 2B). These results suggested that 1.0 mg of siRNA could be loaded to 30 mg GCE carrier completely. Based on the agarose gel
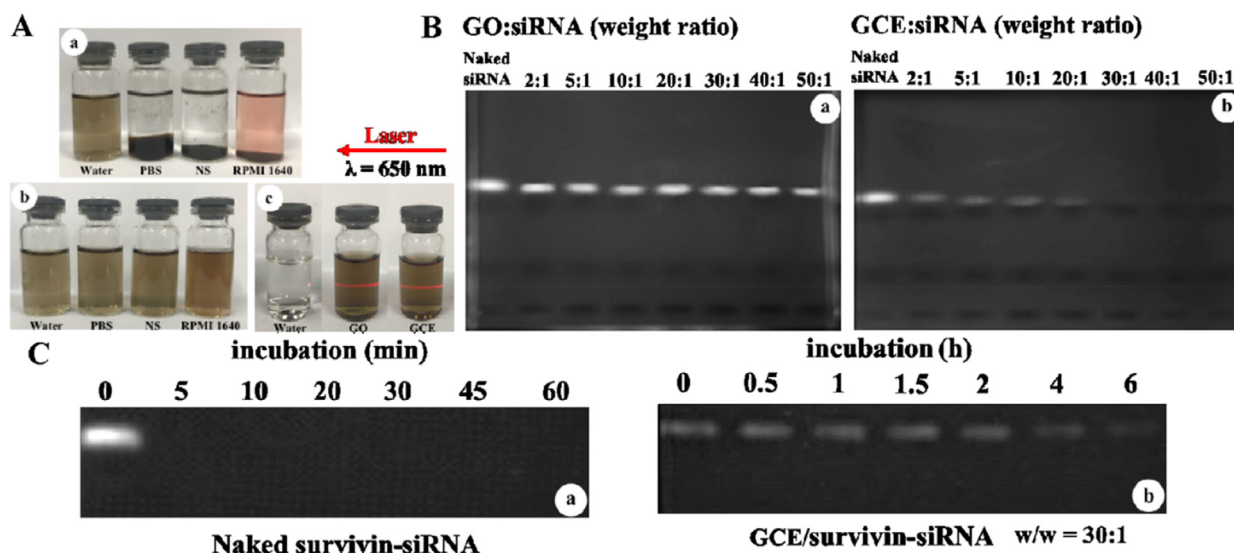
Fig. 2 – Drug loading ability and stability of GCE. (A) The stability and dispersibility of GO (a), GCE (b), Tyndall phenomenon of GO and GCE (c). (B) Agarose gel retardation test of siRNA treated with GO (a) and GCE (b). (C) Degradation of naked siRNA (a) and GCE/siRNA (b) with Heparin and RNase A.
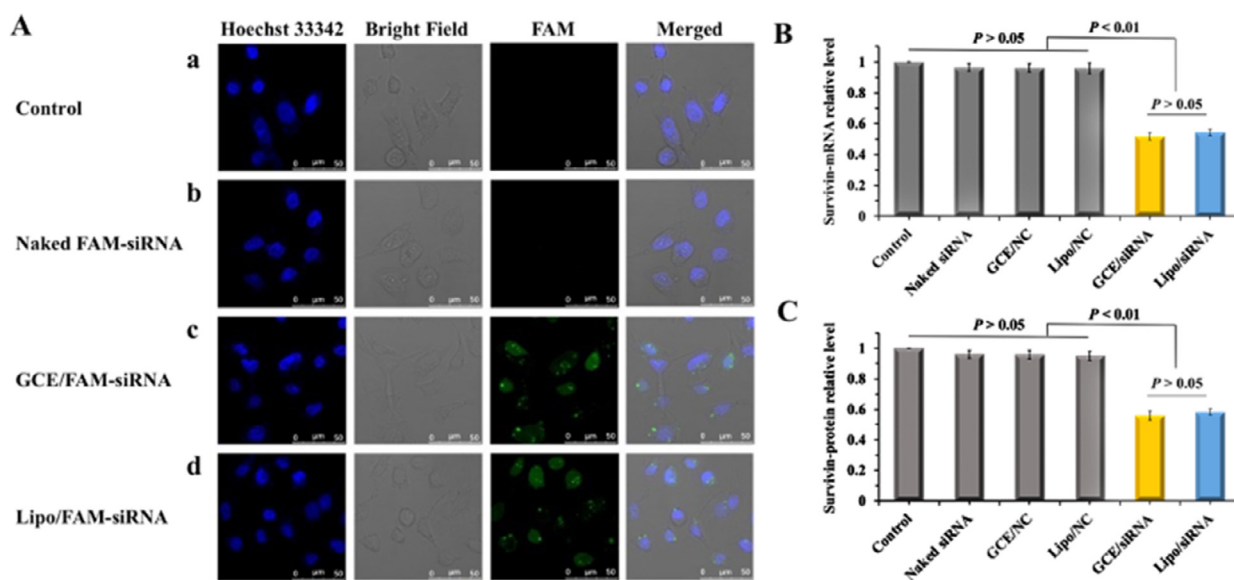

Fig. 3 – Intracellular delivery and gene silencing of GCE/siRNA *in vitro*. (A) Confocal images treated by PBS, naked siRNA, GCE/siRNA, and Lipo/siRNA; siRNA was labled with FAM fluorescent molecule (green) to show the amount of siRNA into cells, and Hoechst 33,342 (blue) for cell nucleus. (B) Survivin-mRNA levels of the MCF-7 cells treated with different survivin-siRNA formulations were tested by RT-PCR. (C) Survivin protein levels treated with different survivin-siRNA formulations were tested by ELISA assay. The cells with no treatment was considered as a control. The data were presented as the mean ± SD, $n = 3$. (For interpretation of the references to colour in this figure legend, the reader is referred to the web version of this article.)

retardation assay, GCE/siRNA nanoparticles by a weight ratio of 30 were used in the following experiments.

The stability of GCE was tested in different solutions (PBS, NS and RPMI-1640 medium). As shown in Fig. 2A, GO was precipitated in all the solutions, while GCE could disperse homogeneously, indicating that the modification could increase the stability of GO. The brilliant stability of

GCE may be due to the increase of the layer resistance effect and the electrostatic shielding effect. Moreover, the result of cumulative release proved that GCE/siRNA had a sustained release effect for siRNA, which could prolong the effect of siRNA *in vivo* (Fig. 4S).

The protective effect of GCE on siRNA was also evaluated by gel retardation assay. The band of siRNA was degraded
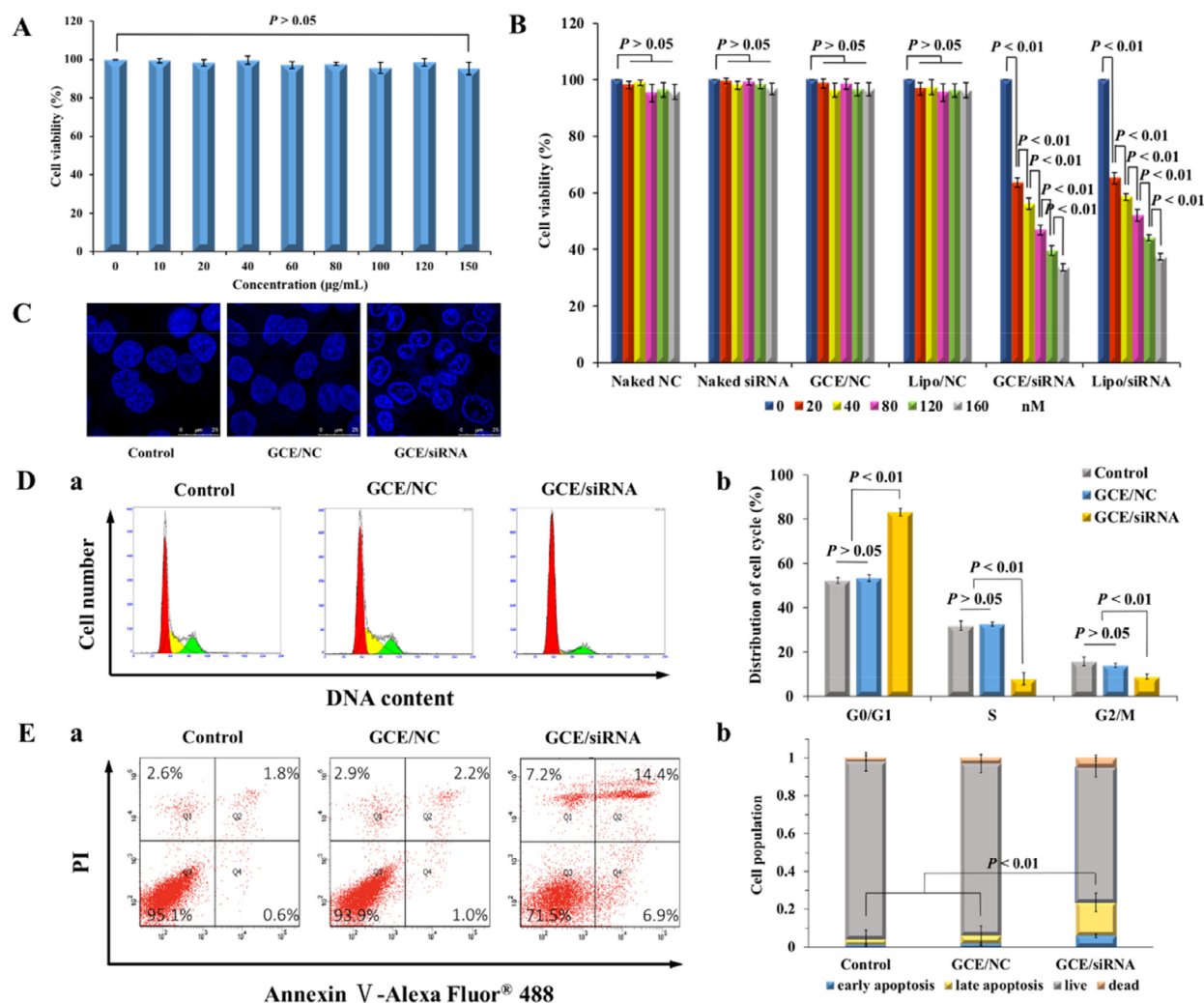
Fig. 4 – Safety of GCE and antiproliferation effect of GCE/siRNA *in vitro*. (A) The cytotoxicity of GCE on MCF-7 cells using MTT method. (B) Anti-proliferation effect of GCE/siRNA in MCF-7 cells. The results were presented as the mean ± SD, $n = 3$. (C) Effect of GCE/siRNA on apoptosis morphology of MCF-7 cells. (D) Cell cycle distribution of MCF-7 cells treated by survivin-siRNA for 48 h. (a) Distribution of MCF-7 cell cycle detected by flow cytometry in different treatment groups. (b) Statistical chart of cell cycle distribution of MCF-7 cells in different treatment groups. (E) The apoptosis of MCF-7 cells induced by siRNA for 48 h. (a) Flow cytometric plot of rate of apoptosis by annexin V and PI staining of MCF-7 cells. (b) Apoptosis rate of MCF-7 cells in different treatment groups. The cells with no treatment was considered as a control. The data were presented as the mean ± SD, $n = 3$.

by RNase A within 5 min. For GCE/siRNA, a bright band of survivin-siRNA could still be observed from GCE/siRNA even after incubating with RNase A for 6 h (Fig. 2C). These results indicated that GCE vector could effectively protect survivin-siRNA from degradation *in vivo*. As it's reported, one of the main elements for a successful siRNA delivery system is protection of siRNA from degradation [48]. The RNase A degradation study suggested that GCE is a promising system for siRNA delivery.

3.3. Intracellular delivery and in vitro gene silencing effect of GCE/siRNA

Efficient cellular uptake is a critical step for the gene silencing effect of survivin-siRNA. FAM-siRNA was applied to trace the siRNA uptake in MCF-7 cells. As shown in Fig. 3A, the green fluorescence of FAM in GCE/siRNA were much stronger than that in control and naked siRNA group. The fluorescence of FAM distributed around cell nucleus. The result also displayed that GCE/siRNA had the same delivery behavior as Lipo/siRNA group (positive control group), suggesting that GCE vector could deliver survivin-siRNA into MCF-7 cells effectively.

The *in vitro* gene silencing effect of GCE/siRNA was confirmed by RT-PCR analysis. Compared with control and negative controls (naked siRNA, GCE/NC, Lipo/NC), the relative amount of mRNA in GCE/siRNA group was downregulated by 48.24% ± 2.50%, and that was lower than Lipo/siRNA group (45.76% ± 1.98%, $P < 0.01$) (Fig. 3B). The results showed that GCE/siRNA downregulate the expression of RNA effectively. The downregulated expression of protein was determined
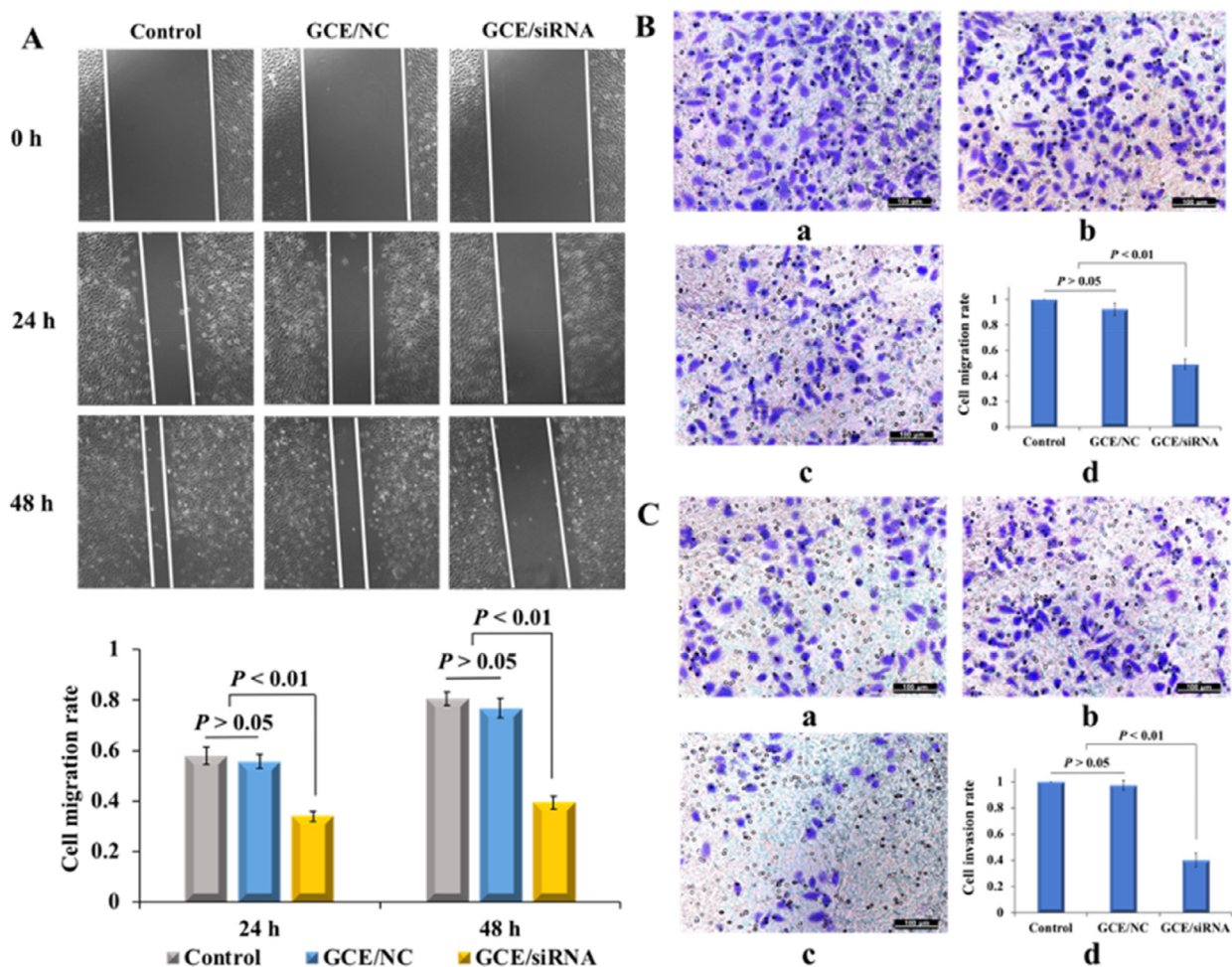
Fig. 5 – Migration and invasion inhibition effects of GCE/siRNA on MCF-7 cells. (A) Effect of survivin-siRNA on MCF-7 cells migration by wound healing assay. (a) Photographs of MCF-7 cells in different treatment groups at 0, 24 and 48 h by wound healing assay. (b) Statistical chart of cell migration rate of MCF-7 cells in different treatment groups. (B) Migration by transwell assay. (a) Control, (b) GCE/NC, (c) GCE/siRNA, (d) Statistical chart of number of migrated MCF-7 cells in different treatment groups. (C) Effect of invasion by transwell assay. (a) Control, (b) GCE/NC, (c) GCE/siRNA, (d) Statistical chart of number of invaded MCF-7 cells in different treatment groups. The cells with no treatment were considered as a control. The data were presented as the mean ± SD, $n = 3$.

by ELISA analysis (Fig. 3C). Compared with the control, the expression level of survivin-protein in GCE/siRNA group was decreased ($P < 0.01$). The downregulation rates of the protein were $44.12\% \pm 3.03\%$ and $41.77\% \pm 1.97\%$ for GCE/siRNA and Lipo/siRNA, respectively. There was no significant difference on protein downregulation rates for GCE/siRNA group and Lipo/siRNA group ($P > 0.05$). The above results showed that GCE/siRNA could regulate the expression of protein.

3.4. In vitro antiproliferation assay

A series of antiproliferation assays were carried out to explore the inhibition effect of survivin-siRNA in MCF-7 cells. Firstly, the toxicity of GCE carriers was tested by MTT assay, suggesting that GCE had no effect on the MCF-7 cells (Fig. 4A). Then, the antiproliferation effect of GCE/siRNA was tested (Fig. 4B). As the increase of siRNA concentration, the survival

rate of MCF-7 cells in GCE/siRNA group decreased significantly, which had the same effect as Lipo/siRNA. The results indicated that GCE/siRNA had excellent antiproliferation effect *in vitro*. Besides, the apoptotic morphology observed by CLSM also suggested that GCE/siRNA treated could make cell nucleus shrinking and irregular (Fig. 4C), which was a typical character of apoptotic nuclear morphology [49,50]. All of these results above indicated that the GCE/siRNA could inhibit MCF-7 cells growth by antiproliferation and cell apoptosis effects.

In order to explore the apoptosis mechanisms of GCE/siRNA, cell apoptosis and cell cycle analysis were performed by FCM. The results of cell cycle were shown in Fig. 4D. As for GCE/siRNA treated group, the G0/G1 proportion of cells increased greatly. The cell cycle analysis suggesting that GCE/siRNA could inhibit cell proliferation by blocking at G0/G1 phase. The results were shown in Fig. 4E. The apoptosis rates in control group and GCE/NC group were $3\%.9 \pm 1.3\%$ and
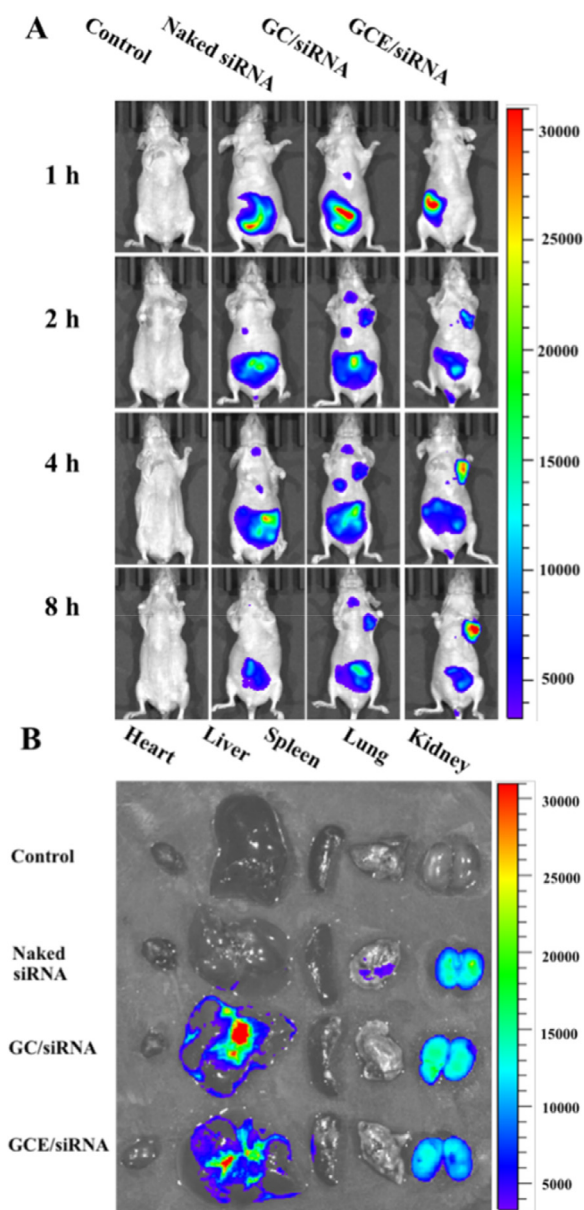
Fig. 6 – In vivo fluorescence image of survivin-siRNA injected into tail of BALB/c nude mice. (A) Images were taken at different time point after tail vein injection. (B) Image of collected organs from each group was taken at 8 h after tail vein injection.

5.8% ± 2.1%, while the apoptosis rate in GCE/siRNA group was increased remarkably to 23.9% ± 2.6%. The results indicated that GCE/siRNA could induce cell apoptosis in MCF-7 cells effectively.

3.5.   Cell migration and invasion assays

It was reported that survivin-siRNA could suppressed tumor growth by inhibiting cell migration and invasion [51,52]. So wound healing assay and transwell assay were performed to evaluate the effects of GCE/siRNA on cell migration and invasion. As shown in Fig. 5A, the migration rate of GCE/siRNA

group was significantly inhibited at 1 d and 2 d ($P < 0.01$). It demonstrated that downregulation of survivin expression could inhibit MCF-7 cell migration. The migration inhibition effect of survivin-siRNA was also confirmed by transwell assay (Fig. 5B). The migration rate of MCF-7 cells treated with GCE/siRNA was 0.49 ± 0.04, which was much lower than that in control and GCE/NC ($P < 0.01$).

In order to confirm the invasion inhibition effect of GCE/siRNA, transwell chamber covered with matrigel was applied to simulate the invasion environment. The cell invasion rate of MCF-7 cells in GCE/siRNA was also lower significantly ($P < 0.01$) (Fig. 5C). All of the results showed that GCE/siRNA inhibit the cell migration and cell invasion by silencing survivin expression.

3.6.   In vivo drug distribution

The successful delivery of survivin-siRNA into tumor tissues is the main step for the anti-tumor effect of survivin-siRNA, so targeting effect and distribution in vivo were investigated in MCF-7 xenograft models. After intravenous injection of NS (Control), naked Cy5-siRNA (Naked siRNA), GC/Cy5-siRNA (GC/siRNA) and GCE/Cy5-siRNA (GCE/siRNA), fluorescence of the tumor-bearing mice was performed at different time points (1, 2, 4 and 8 h). After intravenous injection for 2 h, there was fluorescence in tumor for GC/siRNA and GCE/siRNA groups, and the fluorescence intensity increased gradually (Fig. 6A). It suggested that survivin-siRNA loaded on carriers could accumulate in tumor through the blood circulation system of mice. Interestingly, at 2, 4 and 8 h, the fluorescence intensity of tumor in GCE/siRNA group was higher than that in GC/siRNA group. Compared with GC/siRNA, GCE/siRNA was modified with anti-EpCAM, which is a specific antibody for highly expresses EpCAM molecule on the surface of MCF-7 cells [53]. So it was confirmed that modification with anti-EpCAM ensured the targeting effect of GCE/siRNA in vivo. After 8 h, the mice were executed, and the organs were gotten to observe the siRNA distribution. As shown in Fig. 6B, all of the tested groups had a strong fluorescence in kidney, indicating that the kidney was the main metabolic organ for siRNA. While for GC/siRNA group and GCE/siRNA group, there was also distinct fluorescence in liver. It was speculated that graphene oxide nanoparticles were mainly excreted through bile after liver metabolism. In addition, the fluorescence intensity of the main organs in GCE/siRNA group was weaker than that in GC/siRNA group, which further confirmed that more survivin-siRNA was accumulated in tumor tissue.

3.7.   Tumor inhibition assays

According to the results above, it suggested that GCE/siRNA would have a brilliant anti-tumor effect in vivo, therefore, the tumor inhibition effect of GCE/siRNA was investigated. It could be seen that the tumor inhibition effect of GCE/siRNA was higher significantly ($P < 0.01$), and GCE/siRNA had an equal anti-tumor effect as DOX (Fig. 7A). And as shown in Fig. 7B, the tumor volumes of GCE/siRNA and DOX were smaller than those of control and siRNA groups. In addition, the tumor inhibition rate of GCE/siRNA group 54.74% ± 5.51% were significantly higher than those of siRNA group 4.87 ±
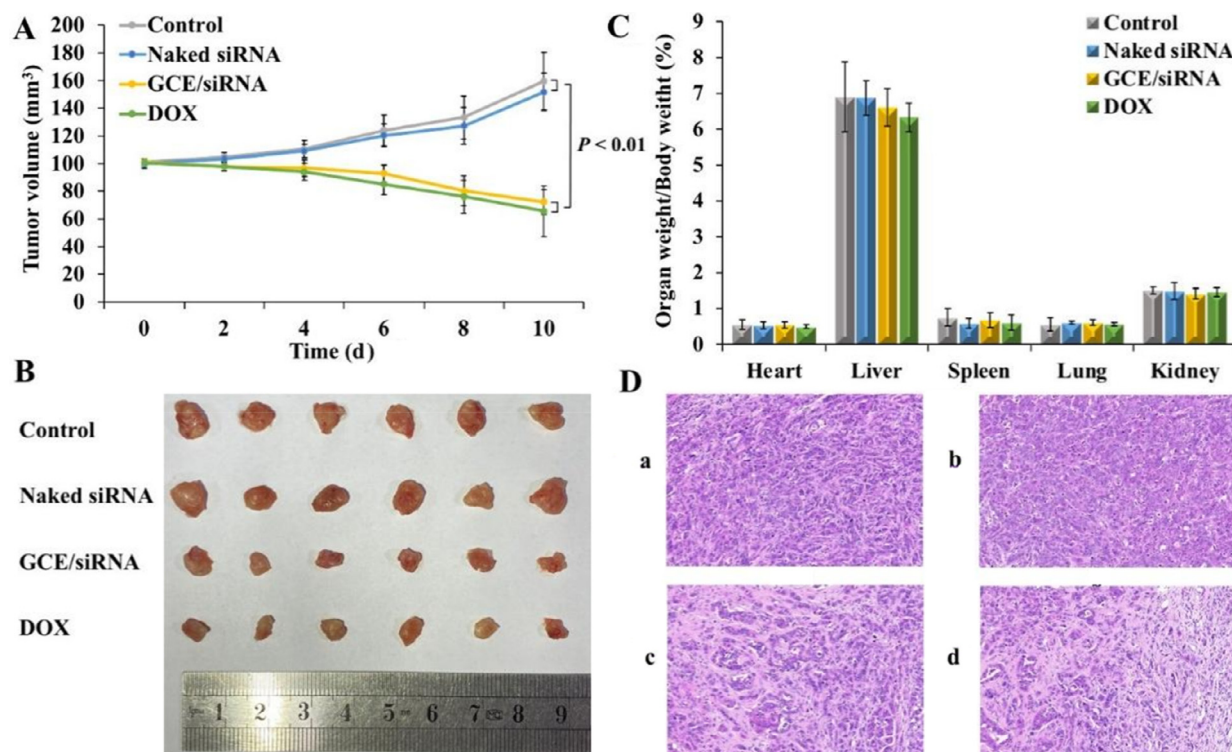
Fig. 7 – *In vivo* tumor therapeutic efficiency of GCE/siRNA. (A) Tumor volume changes of mice were measured every two days. (B) Image of tumors harvested from the mice on the day after the last injection. (C) The ratios of organ weight to body weight. (D) H&E staining of MCF-7 tumor tissues in nude mice injected with (a) NS (Control), (b) naked siRNA, (c) GCE/siRNA, (d) DOX. (100 ×). The data were presented as the mean ± SD, *n* = 6.

8.49%. These results indicated that GCE/siRNA could have a positive therapeutic effect on tumor inhibitory *in vivo*. What's more, according to the ratios of organ to body weight, GCE/siRNA would not induce serious damage to the main organs *in vivo* (Fig. 7C).

H&E staining was applied to revealing the histological change by GCE/siRNA. It was obvious that the tumor cells in control group and naked siRNA group were closely arranged. In GCE/siRNA group, the tumor cells became sparse, and the intercellular space became large, which were the typical characters of necrosis. And this necrosis phenomenon was also observed in DOX group (Fig. 7D). These results showed that GCE/siRNA effectively inhibit the proliferation of MCF-7 tumor by promoting cell apoptosis.

3.8. Safety study in vivo

Since most of siRNA delivery systems are constructed by cationic materials, they may cause serious blood and tissue toxicity after administration *in vivo*. So it is necessary to evaluate the biosafety of siRNA vectors. Firstly, the organs were stained by H&E to explore the organ toxicity of GCE/siRNA. As shown in Fig. 8A, there was no obvious pathological feature in heart, liver, spleen, lung and kidney of each group, suggesting that GCE/siRNA had no obvious toxicity to the main organs *in vivo*. The hemolysis test

also suggested that GCE/siRNA had good biocompatibility. It was safety to RBC even when siRNA increased to a high concentration (160 nM) (Fig. 8B). Since it has been reported that GO could induce hemolysis [54], the hemolysis test proved that proper surface modification could effectively improve the biocompatibility of GO. Besides, blood biochemistry test was carried out to research the hepatic or renal toxicity of GCE/siRNA. As shown in the Fig. 8C, neither the liver function indexes (ALT, AST, ALP, TB and ALB) nor the renal function indexes (CREA, UA and UREA) between treatment groups and control group had any significant difference in function. Moreover, the blood routine analysis was also performed to further prove the blood safety of GCE/siRNA. The results revealed that there was no significant difference in blood indexes between each treatment group and control group (Table 1). It was widely reported that cationic gene drug carriers would induce blood toxicity by hemolysis as well as organic damage after administration *in vivo* [55]. However, the positive charged GCE was demonstrated to be a brilliant biosafety vector both *in vitro* and *in vivo*, which may be due to the non-toxicity and good biocompatibility of CS decorated on GO. According to previous research, CS was a non-toxicity positive material with brilliant biocompatibility, and decorated with CS would significantly reduce toxicity of drug delivery matertials [56]. So the CS modified GCE exhibited adorable biosafety as a gene drug delivery system.
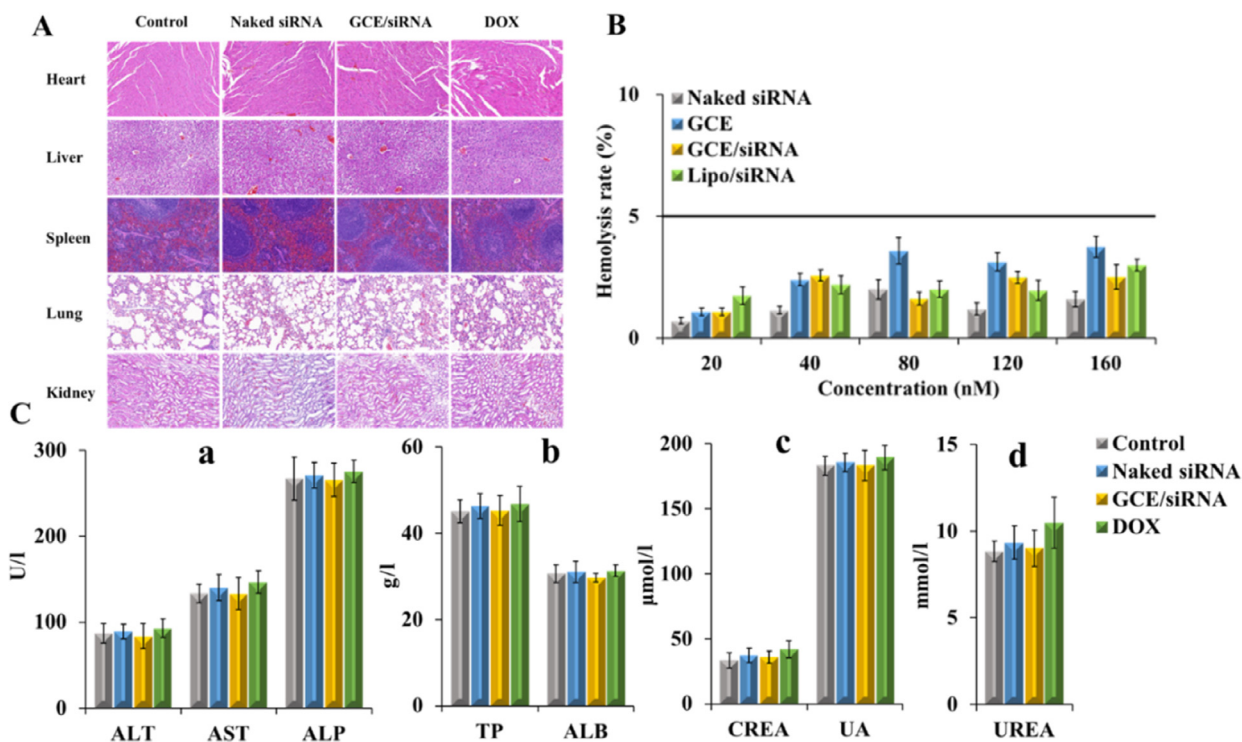
Fig. 8 – Biosafety of GCE/siRNA *in vivo*. (A) H&E staining of the major organs from mice treated with NS (Control), naked siRNA, GCE/siRNA and DOX. (100 x). (B) Hemolysis activity of GCE/siRNA, hemolysis rate was evaluated in rat RBC after treatment with naked siRNA, GCE, GCE/siRNA or Lipo/siRNA. The data were presented as the mean ± SD, $n = 3$. (C) Blood biochemistry data including liver function markers: ALT, AST, ALP, TB and ALB, and kidney function markers: CREA, UA and UREA. The data were presented as the mean ± SD, $n = 5$.

Table 1 – Blood routine test. The data were presented as the mean ± SD, $n = 5$.

	Unit	Control	Naked siRNA	GCE/siRNA	DOX
RBC	10^{12}/l	7.20 ± 0.97	7.22 ± 0.50	7.35 ± 0.75	7.12 ± 0.84
HGB	g/l	134 ± 4	136 ± 4	131 ± 3	129 ± 8
HCT	CV%	40.2 ± 3.1	39.6 ± 3.7	36.2 ± 2.4	38.3 ± 4.7
MCV	fl	54.0 ± 2.3	53.5 ± 1.9	53.3 ± 0.6	53.9 ± 0.6
MCH	pg	17.6 ± 0.2	17.4 ± 0.4	17.3 ± 1.6	17.5 ± 0.9
MCHC	g/l	329 ± 7	327 ± 7	327 ± 4	325 ± 3
RDW	CV%	18.9 ± 1.0	18.1 ± 1.3	18.7 ± 0.6	17.6 ± 0.9
PLT	10^9/l	587 ± 45	583 ± 32	603 ± 42	592 ± 63
WBC	10^9/l	3.5 ± 0.5	3.5 ± 0.7	3.7 ± 0.4	3.3 ± 0.4

RBC: red blood cell, HGB: hemoglobin, HCT: hematocrit, MCV: mean corpuscular volume, MCH: mean corpuscular hemoglobin, MCHC: mean corpuscular hemoglobin concentration, RDW: red blood cell distribution width, PLT: platelet, and WBC: white blood cell.

4.   Conclusion

In summary, a graphene oxide-based siRNA delivery vector was successfully synthesized. The novel siRNA delivery system could not only deliver siRNA into tumor cellular efficiently *in vitro*, but also target siRNA into tumor tissues successfully *in vivo*. GCE exhibited excellent stability under different conditions, and could protect siRNA from degradation by RNase A. The cellular uptake research suggested that GCE could promote the uptake of survivin-siRNA by MCF-7 cells, which had almost the same effect as Lipo^{TM}2000. The efficient delivery effect of GCE/siRNA ensured the gene silencing efficiency of survivin-siRNA. The downregulation rates of survivin-mRNA and survivin-protein had no significant differences between GCE/siRNA and Lipo/siRNA. The *in vitro* experiments proved that GCE/siRNA could suppress MCF-7 cell proliferation, which is attributed to the apoptosis promoting and metastatic inhibition effects of siRNA. Moreover, GCE exhibit a brilliant tumor targeting effect, since the modification of anti-EpCAM. Besides, the toxicity and biosafety research *in vitro* and *in vivo* were carried out. The results indicated that GCE was a safety material, and had no damage to the main organs as a gene delivery system. All of the results in this research depict a novel vector with remarkable gene delivery ability, and also highlight the importance of rational delivery-system design for RNA interference technology in cancer treatment.

Conflicts of interest

The authors report no conflicts of interest. The authors alone are responsible for the content and writing of this article.

Acknowledgments

Supplementary materials

Supplementary material associated with this article can be found, in the online version, at doi:10.1016/j.ajps.2021.04.002.

REFERENCES

[1] Marzbali MY, Khosroushahi AY. Polymeric micelles as mighty nanocarriers for cancer gene therapy: a review. Cancer Chemother Pharmacol 2017;79(4):637–49.

[2] Ylä-Herttuala S, Baker AH. Cardiovascular gene therapy: past, present, and future. Mol Ther 2017;25(5):1095–106.

[3] Alam T, Khan S, Gaba B, Haider MF, Baboota S, Ali J. Nanocarriers as treatment modalities for hypertension. Drug Deliv 2017;24(1):358–69.

[4] Chellappan DK, SSivamb N, Teoh KX, Leong WP, Fui TZ, Chooi K, et al. Gene therapy and type 1 diabetes mellitus. Biomed Pharmacother 2018;108:1188–200.

[5] Fire A, Xu S, Montgomery MK, Kostas SA, Driver SE, Mello CC. Potent and specific genetic interference by double-stranded RNA in Caenorhabditis elegans. Nature 1998;391:806–11.

[6] MVélez A, Fishilevich E. The mysteries of insect RNAi: a focus on dsRNA uptake and transport. Pestic Biochem Physiol 2018;151:25–31.

[7] Reynolds N, Dearnley M, Hinton TM. Polymers in the delivery of siRNA for the treatment of virus infections. Top Curr Chem 2017;375(2):38.

[8] Forbes D, Peppas N. Polycationic nanoparticles for siRNA delivery: comparing ARGET ATRP and UV-initiated formulations. ACS Nano 2014;8(3):2908–17.

[9] Nadithe V, Liu R, Killinger BA, Movassaghian S, Kim NH, Moszczynska AB, et al. Screening nylon-3 polymers, a new class of cationic amphiphiles, for siRNA delivery. Mol Pharm 2015;12(2):362–74.

[10] Whitehead KA, Langer R, Anderson DG. Knocking down barriers: advances in siRNA delivery. Nat Rev Drug Discov 2009;8(2):129–38.

[11] Wang S, Huang R. Non-viral nucleic acid delivery to the central nervous system and brain tumors. J Gene Med 2019;21(7):e3091.

[12] Li J, Liang H, Liu J, Wang Z. Poly (amidoamine) (PAMAM) dendrimer mediated delivery of drug and pDNA/siRNA for cancer therapy. Int J Pharm 2018;546(1–2):215–25.

[13] Wang J, Guo C, Yue T, Yuan Y, Liu X, Kennedy JF. Cationization of ganoderma lucidum polysaccharides in concentrated alkaline solutions as gene carriers. Carbohyd Polym 2012;88(3):966–72.

[14] Inoh Y, Furuno T, Hirashima N, Kitamoto D, Nakanishi M. Synergistic effect of a biosurfactant and protamine on gene transfection efficiency. Eur J Pharm Sci 2013;49(1):1–9.

[15] Wang Y, Luo YL, Chen YF, Lu ZD, Wang Y, Czarna A, et al. Dually regulating the proliferation and the immune microenvironment of melanoma via nanoparticle-delivered siRNA targeting onco-immunologic CD155. Biomater Sci 2020.

[16] Li H, Hao Y, Wang N, Wang L, Jia S, Wang Y, et al. DOTAP functionalizing single-walled carbon nanotubes as non-viral vectors for efficient intracellular siRNA delivery. 2016;23(3):840–8.

[17] Novoselov K, Geim A. The rise of graphene. Nat Mater 2007;6(3):183–91.

[18] Fasolino A, Los JH, Katsnelson MI. Intrinsic ripples in graphene. Nat Mater 2007;6:858–61.

[19] Hummers WS, Offeman RE. Preparation of graphitic oxide. J Am Chem Soc 1958;80(6):1339.

[20] Dreyer DR, Park S, Bielawski CW, Ruoff RS. The chemistry of graphene oxide. Chem Soc Rev 2010;39(1):228–40.

[21] Chiu NF, Huang TY, Lai HC. Graphene oxide based surface plasmon resonance biosensors. Sens Actuators B Chem 2013;197(7):35–42.

[22] Singh DP, Herrera CE, Singh B, Singh S, Singh RK, Kumar R. Graphene oxide: an efficient material and recent approach for biotechnological and biomedical applications. Mater Sci Eng C 2018;86:173–97.

[23] Rao Z, Ge H, Liu L, Zhu C, Min L, Liu M, Fan L, Li D. Carboxymethyl cellulose modified graphene oxide as pH-sensitive drug delivery system. Int J Biol Macromol 2018;107(Pt A):1184–92.

[24] Liu P, Wang S, Liu X, Ding J, Zhou W. Platinated graphene oxide: a nanoplatform for efficient gene-chemo combination cancer therapy. Eur J Pharm Sci 2018;121:319–29.

[25] Jang SC, Kang SM, Lee JY, Oh SY, Vilian AE, Lee I, et al. Nano-graphene oxide composite for *in vivo* imaging. Int J Nanomed 2018;13:221–4.

[26] Yoon J, Lee T, G BB, Jo J, Oh BK, Choi JW. Electrochemical H_2O_2 biosensor composed of myoglobin on MoS_2 nanoparticle-graphene oxide hybrid structure. Biosens Bioelectron 2017;93:14–20.

[27] Jiang L, Su C, Ye S, Wu J, Zhu Z, Wen Y, et al. Synergistic antibacterial effect of tetracycline hydrochloride loaded functionalized graphene oxide nanostructures. Nanotechnology 2018;29(50):505102.

[28] Carrillo C, Suñé JM, Pérez-Lozano P, García-Montoya E, Sarrate R, Fàbregas A, et al. Chitosan nanoparticles as non-viral gene delivery systems: determination of loading efficiency. Biomed Pharmacother 2014;68(6):775–83.

[29] Shen J, Zhang W, Qi R, Mao Z-W, Shen H. Engineering functional inorganic-organic hybrid system advances in siRNA therapeutics. Chem Soc Rev 2018;47(6):1969–95.

[30] Carvalho AM, Cordeiro RA, Faneca H. Silica-based gene delivery systems: from design to therapeutic applications. Pharmaceutics 2020;12(7):649.

[31] Hashemi E, Mahdavi H, Khezri J, Razi F, Shamsara M, Farmany A. Enhanced gene delivery in bacterial and mammalian cells using PEGylated calcium doped magnetic nanograin. Int J Nanomed 2019;14:9879–91.

[32] Loh XJ, Lee TC, Dou Q, Deen GR. Utilising inorganic nanocarriers for gene delivery. Biomater Sci 2016;4(1):70–86.

[33] Baeuerle PA, Gires O. EpCAM (CD326) finding its role in cancer. Br J Cancer 2007;96(3):417–23.

[34] Went PTH, Lugli A, Meier S, Bundi M, Mirlacher M, Sauter G, et al. Frequent EpCam protein expression in human carcinomas. Hum Pathol 2004;35(1):122–8.

[35] Patriarca C, Macchi RM, Marschner AK, Mellstedt H. Epithelial cell adhesion molecule expression (CD326) in cancer: a short review. Cancer Treat Rev 2012;38(1):68–75.

[36] Mashhadi SMY, Kazemimanesh M, Arashkia A, Azadmanesh K, Meshkat Z, Golichenari B, et al. Shedding light on the EpCAM: an overview. J Cell Physiol 2019;234(8):12569–80.

[37] Osta WA, Chen Y, Mikhitarian K, Mitas M, Salem M, Hannun YA, et al. EpCAM is overexpressed in breast cancer and is a potential target for breast cancer gene therapy. Cancer Res 2004;64(16):5818–24.

[38] Du D, Wang L, Shao Y, Wang J, Engelhard MH, Lin Y. Functionalized graphene oxide as a nanocarrier in a multienzyme labeling amplification strategy for ultrasensitive electrochemical immunoassay of phosphorylated p53 (S392). Anal Chem 2011;83(3):746–52.

[39] Wang ZW, Gao YT, Wang ZF, Yan LL, Zhang HJ, Zhao J. Electrochemical research of cadmium on carboxylated graphene electrode. Chem Res Appl 2013;25(8):1078–84.

[40] Bao H, Pan Y, Ping Y, Sahoo NG, Wu T, Li L, et al. Chitosan-functionalized graphene oxide as a nanocarrier for drug and gene delivery. Small 2011;11:1569–78.

[41] Li L, Luo C, Song Z, Reyes-Vargas E, Clayton F, Huang J, et al. Association of anti-HER2 antibody with graphene oxide for curative treatment of osteosarcoma. Nanomedicine 2018;14(2):581–93.

[42] Zordan MD, Mill CP, Riese DJ, Leary JF. A high throughput, interactive imaging, bright-field wound healing assay. Cytom A 2011;79(3):227–32.

[43] Bo C, Wu Q, Zhao H, Li X, Zhou Q. Thymosin α1 suppresses migration and invasion of PD-L1 high-expressing non-small-cell lung cancer cells via inhibition of STAT3-MMP2 signaling. Onco Targ Ther 2018;11:7255–70.

[44] Yang Z, Wang R, Zhang T, Dong X. MicroRNA-126 regulates migration and invasion of gastric cancer by targeting CADM1. Int J Clin Exp Pathol 2015;8(8):8869–80.

[45] Sun Q, Wang X, Cui C, Li J, Wang Y. Doxorubicin and anti-VEGF siRNA co-delivery via nano-graphene oxide for enhanced cancer therapy in vitro and in vivo. Int J Nanomed 2018;13:3713–28.

[46] Wang X, Sun Q, Cui C, Li J, Wang Y. Anti-HER2 functionalized graphene oxide as survivin-siRNA delivery carrier inhibits breast carcinoma growth in vitro and in vivo. Drug Des Devel Ther 2018;12:2841–55.

[47] Li J, Ge X, Cui C, Zhang Y, Wang Y, Wang X, et al. Preparation and characterization of functionalized graphene oxide carrier for siRNA delivery. Int J Mol Sci 2018;19(10):3202.

[48] Kim B, Park JH, Sailor MJ. Rekindling RNAi therapy: materials design requirements for in vivo siRNA delivery. Adv Mater 2019;31(49):e1903637.

[49] Mandelkow R, Gümbel D, Ahrend H, Kaul A, Zimmermann U, Burchardt M, et al. Detection and quantification of nuclear morphology changes in apoptotic cells by fluorescence microscopy and subsequent analysis of visualized fluorescent signals. Anticancer Res 2017;37(5):2239–44.

[50] Ansil PN, Wills PJ, Varun R, Latha MS. Cytotoxic and apoptotic activities of amorphophallus campanulatus (Roxb.) Bl. tuber extracts against human colon carcinoma cell line HCT-15. Saudi J Biol Sci 2014;21(6):524–31.

[51] Li Y, Zhou Y, Zheng J, Niu C, Liu B, Wang M, et al. Downregulation of survivin inhibits proliferation and migration of human gastric carcinoma cells. Int J Clin Exp Pathol 2015;8(2):1731–6.

[52] Ma WH, Liu YC, Xue ML, Zheng Z, Ge YL. Downregulation of survivin expression exerts antitumoral effects on mouse breast cancer cells in vitro and in vivo. Oncol Lett 2016;11(1):159–67.

[53] Schnell U, Cirulli V, Giepmans BNG. EpCAM: structure and function in health and disease. Biochim Biophys Acta 2013;1828(8):1989–2001.

[54] Liao KH, Lin YS, Macosko CW, Haynes CL. Cytotoxicity of graphene oxide and graphene in human erythrocytes and skin fibroblasts. ACS Appl Mater Interfaces 2011;3(7):2607–15.

[55] Kurosaki T, Kitahara T, Kawakami S, Higuchi Y, Yamaguchi A, Nakagawa H, et al. Gamma-polyglutamic acid-coated vectors for effective and safe gene therapy. J Control Release 2010;142(3):404–10.

[56] Worthington KLS, Adamcakova-Dodd A, Wongrakpanich A, Mudunkotuwa IA, Mapuskar KA, Joshi VB, et al. Chitosan coating of copper nanoparticles reduces in vitro toxicity and increases inflammation in the lung. Nanotechnology 2013;24(39):395101.